Irrig Sci (2015) 33:289–302
DOI 10.1007/s00271-015-0466-4

ORIGINAL PAPER

Modeling soil water dynamics in a drip-irrigated intercropping field under plastic mulch

Xianyue Li[1] · Haibin Shi[1] · Jiří Šimůnek[2] · Xuewen Gong[1] · Zunyuan Peng[1]

Received: 4 May 2014 / Accepted: 31 March 2015 / Published online: 10 April 2015

Abstract Intercropping, drip irrigation, and the use of plastic mulch are important management practices, which can, when utilized simultaneously, increase crop production and save irrigation water. Investigating soil water dynamics in the root zone of the intercropping field under such conditions is essential in order to understand the combined effects of these practices and to promote their wider use. However, not much work has been done to investigate soil water dynamics in the root zone of drip-irrigated, strip intercropping fields under plastic mulch. Three field experiments with different irrigation treatments (high *T*1, moderate *T*2, and low *T*3) were conducted to evaluate soil water contents (SWC) at different locations, for different irrigation treatments, and with respect to dripper lines and plants (corn and tomatoes). Experimental data were then used to calibrate the HYDRUS (2D/3D) model. Comparison between experimental data and model simulations showed that HYDRUS (2D/3D) described different irrigation events and SWC in the root zone well, with average relative errors of 10.8, 9.5, and 11.6 % for irrigation treatments *T*1, *T*2, and *T*3, respectively, and with corresponding root mean square errors of 0.043, 0.035, and 0.040 $cm^3\ cm^{-3}$, respectively. The results showed that the SWC in the shallow root zone (0–40 cm) was lower under non-mulched locations than under mulched locations, irrespective of the irrigation treatment, while no significant differences in the SWC were observed in the deeper root zone (40–100 cm). The SWC in the shallow root zone was significantly higher for the high irrigation treatment (*T*1) than for the low irrigation treatment, while, again, no differences were observed in the deeper root zone. Simulations of two-dimensional SWC distributions revealed that the low irrigation treatment (*T*3) produced serious severe water stress (with SWCs near the wilting point) in the 30–40 cm part of the root zone, and that using separate drip emitter lines for each crop is well suited for producing the optimal soil water distribution pattern in the root zone of the intercropping field. The results of this study can be very useful in designing an optimal irrigation plan for intercropped fields.

Introduction

Intercropping is the agricultural practice of growing two or more crops side by side in one field. For example, a deep-rooted crop can be planted with a shallow-rooted crop or a tall crop with a shorter crop. One-third of all cultivated land in China is used with an intercropping technique (Zhang and Li 2003) because when compared to monoculture, this management practice largely improves water-use efficiency (WUE) (Tanwar et al. 2014), nitrogen-use efficiency (Rowe et al. 2005), light- and radiation-use efficiency (Awal et al. 2006), and land-use efficiency (Dhima et al. 2007; Tanwar et al. 2014). Intercropping has played an important role in increasing the crop production and farmers' income in many countries, including China (Zhang et al. 2007), India

Communicated by N. Lazarovitch.

✉ Xianyue Li
Lixianyue80@126.com

✉ Haibin Shi
Shb@imau.edu.cn

✉ Jiří Šimůnek
Jiri.Simunek@ucr.edu

[1] College of Water Conservancy and Civil Engineering, Inner Mongolia Agricultural University, Huhhot 010018, China

[2] Department of Environmental Sciences, University of California Riverside, Riverside, CA 92521, USA

(Singh et al. 2013), Egypt (Schader et al. 2005), Malawi (Makumba et al. 2006), and the United States (Parajulee et al. 1997). However, the spatial root distribution, root water uptake, and crop water requirements of two crops in an intercropping field are different compared to monoculture, displaying a non-uniform soil water pattern and crop competition for water and nutrients. Additionally, different crops have different water requirements and need different irrigation amounts at different times in order to increase WUE.

In the Hetao Irrigation District, in the Yellow River basin of Northwest China, water scarcity is the most critical factor restricting agricultural development (Xu et al. 2010). Additionally, the traditional flood irrigation technique produces very low WUE and can hardly resolve the problem of inconsistent water requirements of two crops in an intercropping field. On the other hand, drip irrigation can precisely control the irrigation amount, increase crop yields, reduce water loss (Yaghi et al. 2013), and reduce the risk of soil degradation and salinity (e.g., Keller and Bliesner 1990; Burt and Isbell 2005). Additionally, drip irrigation can easily be operated to account for the different irrigation requirements of the two crops.

Although soil water dynamics was investigated by several scientists for either intercropping fields (e.g., Sampathkumar et al. 2012) or mulched drip irrigation (e.g., Wang et al. 2014), it has not been studied in a system that couples both intercropping and mulched drip irrigation. Soil water dynamics in the root zone under such conditions is very complex, and its understanding is critical for optimizing irrigation management. It is thus important to investigate soil water dynamics under such conditions before promoting the complex management of intercropping, mulching, and drip irrigation agro-techniques.

Although many scientists have studied soil water dynamics in drip-irrigated fields (e.g., Hussein et al. 2011; Ityel et al. 2011; Badr and Abuarab 2013), it is still difficult to design strategies optimizing irrigation amounts, irrigation frequencies, and emitter depths to obtain the highest WUE (Kandelous et al. 2012). The use of computer simulations with validated mathematical models to optimize management practices is a fast and inexpensive approach that has received a lot of attention during the last few decades. In general, there are two types of approaches for simulating the soil water distribution in the drip-irrigated field. One approach is based on the analytical solutions of the governing flow equation, such as the solution of Philip (1984) used in the WetUp model (Cook et al. 2003). Another, more widely used approach is based on the numerical solution of the Richards equation, such as in the HYDRUS (2D/3D) (Šimůnek et al. 2008), Drip-Irriwater (Arbat et al. 2013), or APRI (Zhou et al. 2007) models.

Because of the flexibility of HYDRUS (2D/3D) to accommodate different types of boundary conditions and the root uptake of water and nutrients, and because of its ease of use due to a graphical, user-friendly interface, the model has been widely and successfully used to simulate water movement under drip irrigation in many studies (e.g., Cote et al. 2003; Skaggs et al. 2004; Lazarovitch et al. 2009; Kandelous et al. 2012; Abou Lila et al. 2013; Dabach et al. 2013). For example, Skaggs et al. (2004) compared experimental soil water distributions for drip irrigation with different irrigation amounts and different irrigation durations (20, 40, and 60 L m^{-1} of applied water) with the results of numerical simulations with HYDRUS (2D/3D), in which the soil hydraulic properties were obtained using pedotransfer functions (Schaap et al. 2001). Their results supported the use of HYDRUS (2D/3D) as an important tool for investigating and designing drip irrigation management practices. Although higher irrigation frequencies were suggested in the literature to be a better drip irrigation practice (Assouline et al. 2006), the numerical simulations by Abou Lila et al. (2013) showed that the lower irrigation frequency actually produced a bigger wetted soil volume without an increase in water percolation below the plant roots. Skaggs et al. (2010) evaluated the effects of the application rate, pulsed water applications, and the antecedent water content on the spreading of water from drip emitters using both field experimental data and numerical HYDRUS (2D/3D) simulations. Their results showed that it was mainly the soil texture and the antecedent water content that determined the spreading and distribution of soil water, while irrigation frequency and flow rate had only very little impact (Skaggs et al. 2010). Dabach et al. (2013, 2015) used HYDRUS (2D/3D) to optimize the irrigation threshold, i.e., the pressure head at a selected location, which triggers irrigation when reached; the placement of the triggering location; and the amount of irrigation water applied during one irrigation episode, in order to increase WUE.

Few studies have been carried out for drip irrigation under mulched conditions (e.g., Liu et al. 2013; Wang et al. 2014). For example, Liu et al. (2013) introduced a concept of a partitioning coefficient to describe the effect of plastic mulch on prevention of evaporation. They used the numerical HYDRUS (2D/3D) model to simulate temporal variations in soil water contents (SWC) in a drip-irrigated cotton field under plastic mulch. However, they only calibrated the model (e.g., Liu et al. 2013; Wang et al. 2014) and did not evaluate the effect of the presence or absence of mulching on the SWC distribution.

In intercropping fields, it may be necessary to use different irrigation practices than in monoculture in order to

satisfy different water requirements of two crops. Consequently, the numerical model must accommodate more complicated boundary conditions and root distribution patterns existing in intercropping fields. Sampathkumar et al. (2012) used experimental data to evaluate soil water movement in a drip-irrigated intercropping field under plastic mulch, without comparing the experimental data with the results of a numerical model. On the other hand, De Silva et al. (2008) used HYDRUS (2D/3D) to numerically evaluate root water uptake and soil water movement in a region with a mixture of natural vegetative cover (i.e., trees and grasses), and concluded that different irrigation amounts and frequencies should be used for different plant species in irrigated strip intercropping fields. However, it is difficult to collect information about complex boundary conditions and other operational parameters required by a numerical model for intercropping fields. On the other hand, when the numerical model is calibrated, it can provide a fast and inexpensive approach for investigating soil water dynamics in a drip-irrigated intercropping field under plastic mulch.

The main objectives of this study were (i) to calibrate and validate the HYDRUS (2D/3D) model using the experimental data, (ii) to evaluate the soil water distribution under a mulched drip irrigation system in an intercropping field, and (iii) to compare soil water distributions under different irrigation practices.

Table 1 Design of different irrigation treatments

Treatment	Irrigation amount (mm per irrigation event)	
	Tomato	Corn
*T*1	22.5	30
*T*2	16.5	22.5
*T*3	10.5	15

Materials and methods

Field experiment

The field experiment was carried out from April 1 to September 26, 2012 at the Dunkou Agroecosystem Experimental Station (40°20′15″N, 107°1′45″E, altitude 2004 m), located in the western Hetao Irrigation District, in the Yellow River basin of Northwest China. Average annual precipitation is 198 mm, and average annual evaporation from a free water surface is 2460 mm. The main soil texture in the region is sandy clay loam. The groundwater table during our study was between 73 and 232 cm deep, with the average depth of 134 cm during the crop growth period.

Drip lines were laid out in a "one drip line, one mulch, two crop rows" pattern (i.e., two rows of crops were irrigated with one drip line and mulched with a 70-cm-wide plastic mulch). The drip tape diameter was 16 mm, the wall thickness 0.4 mm, and the discharge rate of the pressure-compensated emitter was 2.4 L h^{-1} at a line pressure of 50 kPa. The strip intercropping consisted of four rows of tomato and two rows of corn. Three irrigation treatments with different (low *T*3, moderate *T*2, and high *T*1) irrigation amounts were used (Table 1), and each was replicated three times in a completely randomized block design of nine plots. While the *T*1 treatment was meant to represent a control, full irrigation treatment, the *T*2 and *T*3 treatments represented moderate and severe deficit irrigations. A compound fertilizer (18 % N, 46 % P_2O_5, and 1.5 % SO_4^{2-}) of 350 kg ha^{-2} was uniformly applied to the plots before sowing. Drip tapes with an emitter spacing of 30 cm and a length of 22 m were placed between two rows of tomatoes and corn, providing water and fertilizer for two adjacent rows of plants. The cropping pattern is shown in Fig. 1. Each treatment had two water meters (with a precision of 0.001 m^3) to control irrigation amounts.

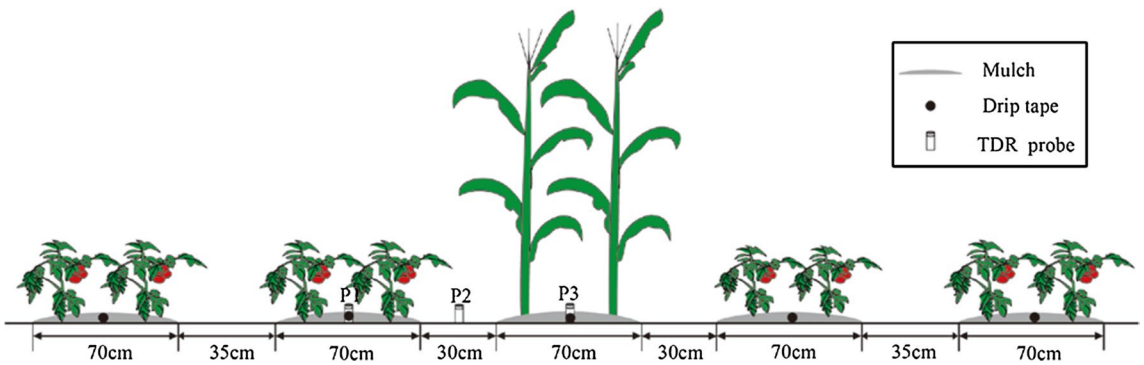

Fig. 1 Schematic showing the cropping pattern (with two double rows of tomatoes and one double row of corn), the arrangement of drip tapes, and the locations of TDR probes and surface mulch

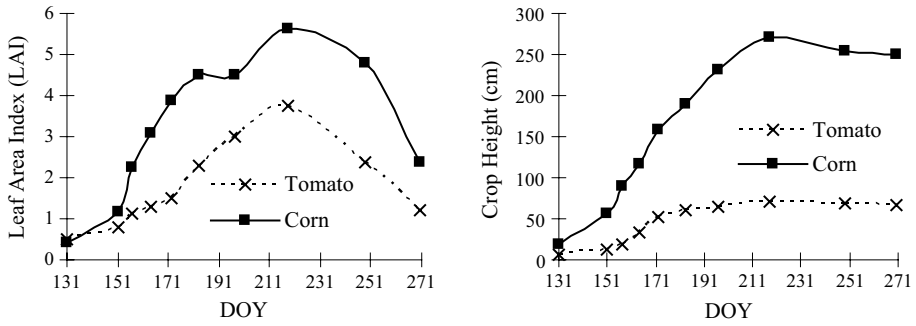

Fig. 2 Leaf area index (LAI) and the crop height of tomato and corn during the growing season

Corn was planted on day of year (DOY) 111, and tomatoes were transplanted on DOY 131. After transplanting, all three fields with different irrigation treatments received a large flood irrigation (about 55 mm) on DOY 132. Different irrigation amounts (high *T*1, moderate *T*2, and low *T*3) were then adopted for tomatoes and corn in the same irrigation treatment (Table 1). Drip irrigation was applied on DOY 167, 175, 190, 196, 199, and 214 to both crops. Since tomatoes were harvested on DOY 221, there was no irrigation applied to the tomato strip after this date. Corn received two additional irrigations on DOY 222 and 228, since it was harvested on DOY 270.

Meteorological data, including solar radiation (S-LIB-M003), photosynthetically active radiation (S-LIA-M003), air temperature and relative humidity (S-THB-M002), air pressure (S-BPA-CM10), wind speed (S-WCA-M003), and precipitation (S-BPA-CM10), were collected at the meteorological station (HOBO, USA) located approximately 500 m from the experimental field. Data were recorded at 1-h intervals, stored in a datalogger (H21-001 DT-80), and regularly downloaded. Reference crop evapotranspiration (ET_0) was calculated using the Penman–Monteith equation (Allen et al. 1998). The SWC was measured using TDR probes (TRIME-PICO-IPH, IMKO GmbH, Germany), which were installed between two rows of tomatoes (*P*1), in the bare section between rows of tomatoes and corn (*P*2), and between two rows of corn (*P*3) in each treatment plot (Fig. 1). TDR measurements were taken once every 5 days at soil depths of 0–10, 10–20, 20–40, 40–60, 60–80, and 80–100 cm. Additional gravimetric measurements were used to verify TDR measurements (Skaggs et al. 2004). The leaf area and the plant height were regularly measured using the leaf area meter (Li-3000, LI-COR, USA) and a tape (the accuracy is about 0.1 cm) (Gao et al. 2010). The leaf area index (LAI), displayed in Fig. 2, was then calculated using the FAO method (Allen et al. 1998).

Data about the horizontal and vertical distributions of crop roots were obtained by digging a soil transect on the experimental site (Gao et al. 2010) on June 6, June 22, July 21, and August 20. The working surface of the soil profile was smoothed, the face of the pit was trimmed to be vertical, and then the vertical plane was divided into square, 5 × 5 cm cells between the tomato strip (*P*1) and the corn strip (*P*3). The entire sampling area was 100 × 100 cm. The sample volumes were 125 cm^3. Root samples were collected and washed off using a root washing machine (Delta-T, CSIRO, Australia). The root length was measured using the root system scanner (Perfection4870photo, Epson, Japan) and then analyzed using the WinRHIZO software. The root length density was calculated (Gao et al. 2010), and the average of the last three measurements was used as an input in HYDRUS (2D/3D) during the second simulation period (explained below).

Numerical model

Drip irrigation is a fully three-dimensional (3D) flow problem (Kandelous et al. 2011). However, under certain conditions, the effects of individual emitters along the drip line can be neglected, and the problem of drip irrigation can be considered as a line source, with infiltration and redistribution being two-dimensional processes (Skaggs et al. 2004; Kandelous et al. 2011; Liu et al. 2013). Although, in general, wetting patterns mainly depend on the emitter's spacing, irrigation duration, initial SWC, and soil hydraulic properties (Skaggs et al. 2004, 2010), the principal concerns of this study are the effects of mulching and different crops on SWC distributions. The HYDRUS (2D/3D) code (Šimůnek et al. 2008) was used to evaluate collected experimental data. HYDRUS (2D/3D) uses the Galerkin finite element method to numerically solve the governing equation (Richards 1931) for variably saturated water flow:

$$\frac{\partial \theta(h)}{\partial t} = \frac{\partial}{\partial x}\left[K(h)\frac{\partial h}{\partial x}\right] + \frac{\partial}{\partial z}\left[K(h)\frac{\partial h}{\partial z} + K(h)\right] - S(h) \quad (1)$$

where θ is the volumetric soil water content ($cm^3\ cm^{-3}$); h is the pressure head (cm); $K(h)$ is the unsaturated hydraulic conductivity (cm day^{-1}); t is time (day); x and z are the horizontal and vertical coordinates (cm), respectively; and S is the sink term (day^{-1}). The root water extraction S was

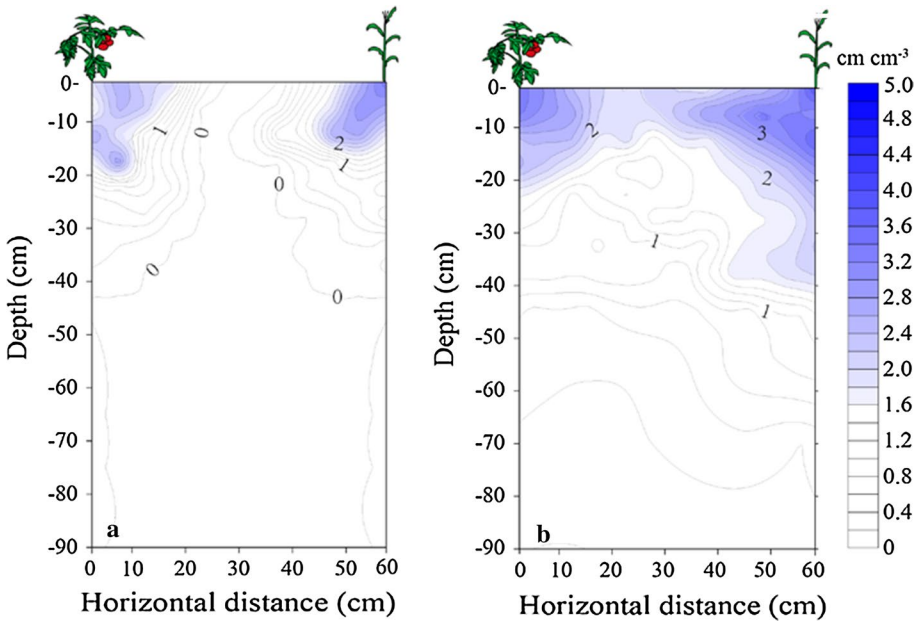

Fig. 3 Average measured spatial root distribution during two simulation periods: **a** DOY 111–138 and **b** DOY 139–270

computed according to the Feddes model (Feddes et al. 1978):

$$S(h) = \tau(h) \cdot \beta(x,z) \cdot T_p L_t \tag{2}$$

where T_p is the potential transpiration rate (cm day^{-1}), L_t is the surface length associated with transpiration (cm), $\beta(x,z)$ is the root water uptake distribution function (cm^{-2}), and $\tau(h)$ is the root water uptake stress reduction function ($0 < \tau < 1$), which includes the following parameters: (a) P_0 and P_{Opt} are the pressure heads, below which roots start extracting water from the soil and roots start extracting water at the maximum possible rate, respectively; (b) P_{2H} and P_{2L} are the limiting pressure heads, below which roots can no longer extract water at the maximum rate (assuming potential transpiration rates r_{2H} and r_{2L}, respectively); and (c) P_3 is the pressure head, below which root water uptake ceases (the wilting point). The following parameter values for corn were adopted from the HYDRUS (2D/3D) database (Šimůnek et al. 2006; Wesseling and Brandyk 1985): $P_0 = 15$ cm, $P_3 = -8000$ cm, $P_{Opt} = -30$ cm, $P_{2H} = -325$ cm, $P_{2L} = -600$ cm, $r_{2H} = 0.5$ cm day^{-1}, and $r_{2L} = 0.1$ cm day^{-1}.

The standard version of HYDRUS (2D/3D) permits the use of the root water uptake stress reduction function for only one crop, while in the intercropping system there are two types of crops with different capacities of root water uptake and with different sensitivities to environmental stresses (e.g., saturation or salinity). We have resolved this problem by considering root water uptake in the model to be directly proportional to the crop root distribution, and thus by adjusting the spatial root distribution in the soil profile, we can affect root water uptake from different parts of the soil profile as well (similarly as done by De Silva et al. 2008). We introduced the ratio of root water uptake per unit root length between corn and tomato (k), assuming that k was identical to the ratio of potential transpirations between corn and tomato monoculture. The ratio k was found to be about 0.96 based on the ratio of crop coefficients during the growing season of corn and tomato (Allen et al. 1998). The region was equally divided into two parts, and the root distribution of a tomato strip was multiplied by k. Since HYDRUS (2D/3D) cannot model root growth, the entire simulation was divided into two parts (Fig. 3). During earlier times, between DOY 111–138, the root zone of both crops was small and did not intersect each other. During later times, between DOY 139–270, in which roots quickly developed and heavily overlapped, there were higher crop transpiration rates and a larger effect of root distributions on the soil water dynamics. The average root distribution during this time period was adopted in calculations in order to reduce the error of not considering a dynamic root growth (Fig. 3).

The HYDRUS (2D/3D) software was easily parameterized as the root distribution is internally normalized (Liu et al. 2013). We assumed that the root length was a relative value equal to 1.0 in the 10 × 10 cm square directly beneath the corn stem. The relative root length in other areas, Root(x, z), was calculated as:

$$\mathrm{Root}(x,z) = \frac{\sigma(x,z)}{\sigma_0} \tag{3}$$

where Root(x, z) is a characteristic value of a normalized, dimensionless spatial distribution of the root length, σ_0 is the root length in the 10 × 10 cm square directly beneath

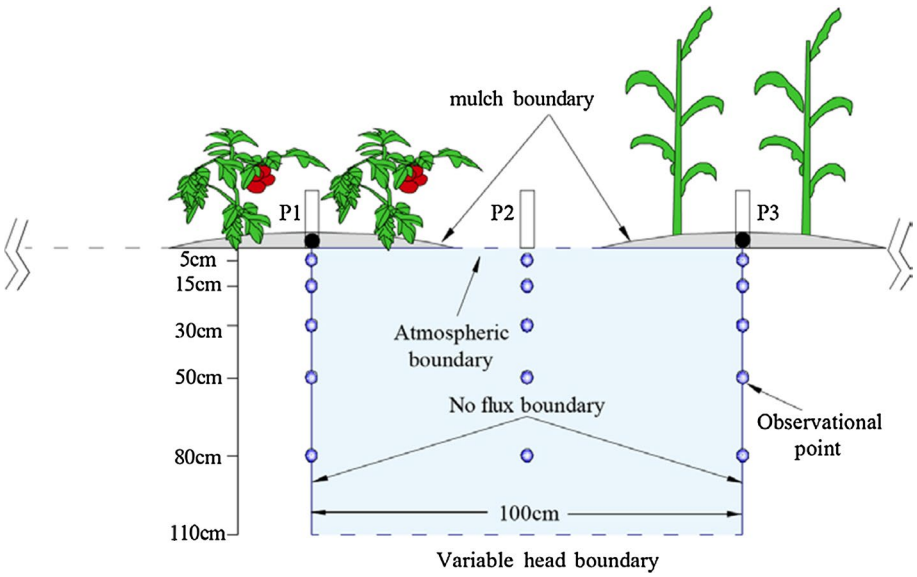

Fig. 4 Schematic of the flow domain and boundary conditions used in the HYDRUS (2D/3D) simulations

the corn stem (cm), and $\sigma(x, z)$ is the root length in other squares (cm). In the HYDRUS (2D/3D) software, the spatial root distribution function assigned to each node, $\beta(x, z)$, is a normalized relative root length (Šimůnek et al. 2006):

$$\beta(x,z) = \frac{\text{Root}(x,z)}{\int_{\Omega} \text{Root}(x,z)d\Omega} \tag{4}$$

where Ω is the root zone domain. Additionally, the soil water content distribution at the end of the first simulation period was used as the initial soil water content distribution for the second simulation period.

Initial and boundary conditions

The initial spatial SWC distribution was estimated based on samples taken from the intercropping field on DOY 110. We assumed that the initial SWC was uniform in the horizontal direction and linearly varied with depth, from about $\theta = 0.18$ cm^3 cm^{-3} at the soil surface to about $\theta = 0.39$ cm^3 cm^{-3} at the bottom of the simulated region (110 cm depth).

Fifteen observation points were defined in HYDRUS (2D/3D) that were located at depths of 5, 15, 30, 50, and 80 cm at three horizontal locations in the middle of the tomato strip (*P*1), bare strip (*P*2), and corn strip (*P*3), as shown in Fig. 4. The simulation was carried out for 160 days. The horizontal width of the flow domain was set to 100 cm, which was the spacing between two lateral drip emitters in the tomato and corn strips. The vertical size of the flow domain was fixed at 110 cm.

The "No Flow" boundary condition was used at vertical sides of the flow domain. The upper boundary was divided into the no-mulch section in the middle 30 cm, where the "Atmospheric" boundary condition was used (Neuman et al. 1974), and the mulch section, where the "Time-Variable Flux" boundary condition (35 cm on each side) was imposed. The "Time-Variable Pressure Head" boundary condition was imposed at the bottom of the transport domain where the pressure head that was measured at regular intervals was imposed. It should be noted that to fully account for complex conditions at the soil surface, the surface energy balance should be solved for each section of the soil surface (e.g., plastic mulch), taking into account different properties of different sections of the soil surface (such as albedo). However, since such option is currently not available in HYDRUS (2D/3D), the approach described below was adapted instead.

Reference crop evapotranspiration (ET_0) was calculated using the Penman–Monteith equation (Allen et al. 1998) during the experimental period by using collected meteorological data. Daily potential evapotranspiration (ET_p) (Fig. 5), required by the model, was obtained by multiplying ET_0 with the crop coefficient (K_c) (Allen et al. 1998):

$$ET_p = K_c \cdot ET_0 \tag{5}$$

where K_c is the synthetic crop coefficient for an intercropping field as recommended by the FAO 56 paper (Allen et al. 1998), which can be calculated as follows:

$$K_c = \frac{f_1 h_1 K_{c1} + f_2 h_2 K_{c2}}{f_1 h_1 + f_2 h_2} \tag{6}$$

where f_1 and f_2 are fractions of the soil surface planted by tomatoes and corn in an intercropping field, i.e., 0.67 and 0.33, respectively; h_1 and h_2 are the heights of tomato and corn, respectively (Fig. 2); and K_{c1} and K_{c2} are crop coefficients for tomato and corn under monoculture conditions, i.e., 1.15 and 1.20, during the middle growth stage, and

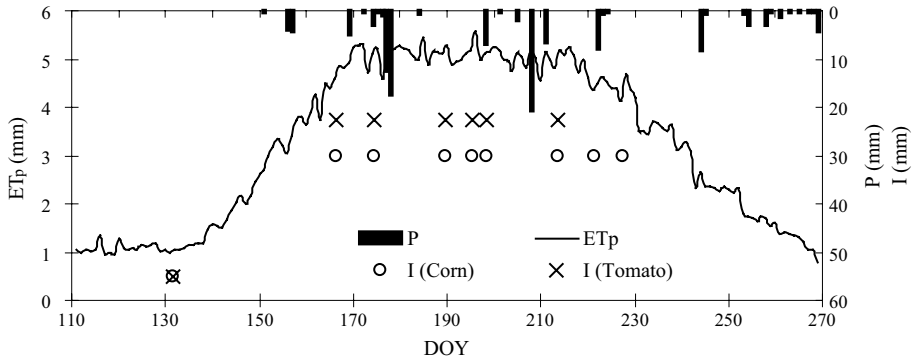

Fig. 5 Potential evapotranspiration (ET_p), precipitation (P), and irrigation (I) for treatment $T1$ during the entire growing season. Note that irrigation amounts for tomato and corn are different, and that there are two additional corn irrigations on DOY 222 and DOY 228

Table 2 Parameters of the van Genuchten model of soil hydraulic properties used in the study (value—optimized value, S. E.—standard error)

Soil layers (cm)	θ_r (cm^3 cm^{-3})		α (1/cm)		n (−)		θ_s (cm^3 cm^{-3})	K_s (cm day^{-1})	l
	Value	S. E.	Value	S. E.	Value	S. E.			
0–20	0.083	0.01	0.054	0.016	1.20	0.03	0.472	170	0.5
20–110	0.092	0.02	0.101	0.025	1.16	0.02	0.484	306	0.5

0.7–0.9 and 0.35–0.6 at the later growth stage, respectively. The FAO 56 paper recommends reducing these values by 10–30 % under plastic mulch conditions. A reduction of 15 % was adopted in our study, and the crop coefficients were considered for tomato and corn ($K_{c\text{-}ini}$) with values of 0.2 and 0.3 at the initial stage, 0.98 and 1.02 at the middle stage ($K_{c\text{-}mid}$), and 0.6 and 0.3 at the later stage ($K_{c\text{-}end}$), respectively. Daily potential evapotranspiration (Fig. 5) was then divided into potential transpiration (T_p) and potential evaporation (E_p), as required by HYDRUS (2D/3D), as follows (Campbell and Norman 1989):

$$T_p = (1 - e^{-k \cdot LAI})ET_p \tag{7}$$

$$E_p = ET_p - T_p \tag{8}$$

where k is the radiation extinction coefficient, which is 0.45 for tomato (Cavero et al. 1998) and 0.49 for corn (Lindquist et al. 2005), and LAI is the leaf area index (Fig. 2).

Evaporation should theoretically be completely prevented when plastic mulch is used. However, due to the aging of plastic, there will always be some evaporation. The potential evaporative flux trough plastic mulch can be calculated according to Liu et at. (2013) as:

$$E_{mulch} = C_p \cdot E_p \tag{9}$$

where E_{mulch} is the evaporative flux through the mulching boundary and C_p is a partitioning coefficient of plastic mulch. According to Liu et al. (2013), its lowest value is 0.07.

The two drip emitters were represented as quarter circles with a 0.8-cm radius located in upper corners of the flow domain (Fig. 4). During irrigation, fluxes of drip emitters were described in HYDRUS (2D/3D) as:

$$\varphi = \frac{Q}{L \times 2\pi R} \tag{10}$$

where φ is the input irrigation flux (cm day^{-1}), Q is the discharge rate (2.4 L h^{-1}), R is the radius of the drip emitter (0.8 cm), and L is the spacing between drip emitters (30 cm). The following values of φ were used for the two crops and three irrigation treatments: 31.35 cm day^{-1} for tomato and 41.79 cm day^{-1} for corn for treatment $T1$, 22.99 and 31.35 cm day^{-1} for treatment $T2$, and 14.63 and 20.90 cm day^{-1} for treatment $T3$, respectively.

Soil hydraulic parameters

Soil hydraulic properties characterizing soil water retention and hydraulic conductivity were described using the analytical functions of van Genuchten (1980) as follows:

$$S_e(h) = \frac{\theta(h) - \theta_r}{\theta_s - \theta_r} = \frac{1}{(1 + |\alpha h|^n)^m} \quad (m = 1 - 1/n) \tag{11}$$

$$K(\theta) = K_s S_e^l [1 - (1 - S_e^{1/m})^m]^2 \tag{12}$$

where S_e is the relative saturation; K_s is the saturated hydraulic conductivity (cm day^{-1}); θ_s and θ_r are the saturated and residual water contents, respectively (cm^3 cm^{-3}); and n, α, l (0.5) are empirical shape factors (Table 2).

The saturated hydraulic conductivity was determined using the constant head method (Booltink et al. 1991), and the saturated soil water content was measured gravimetrically. The inverse approach was used to optimize parameters (θ_r, n, α) and to calibrate the HYDRUS (2D/3D) model (Hopmans et al. 2002; Lazarovitch et al. 2007). The SWC measured at $P1$ and $P2$ locations of treatment 2 between

DOY 60 and DOY 124 was used to calibrate the van Genuchten–Mualem parameters using the Levenberg–Marquardt nonlinear minimization method.

Model performance

The model performance was evaluated using the root mean square error (RMSE) (e.g., Skaggs et al. 2004; Kandelous et al. 2011), the mean absolute error (MAE) (e.g., Doltra and Muñoz 2010), and the mean relative error (MRE) (e.g., Cook et al. 2003; Zhou et al. 2007):

$$\mathrm{RMSE} = \left[\frac{1}{n}\sum_{i=1}^{n}(P_i - O_i)^2\right]^{1/2} \tag{13}$$

$$\mathrm{MAE} = \frac{1}{n}\sum_{i=1}^{n}|P_i - O_i| \tag{14}$$

$$\mathrm{MRE} = \frac{\frac{1}{n}\sum_{i=1}^{n}|P_i - O_i|}{O_i} \times 100\,\% \tag{15}$$

where P_i is the predicted value, O_i is the observed value, and n is the number of compared values.

Results and discussion

Calibration and validation

The $T2$ treatment data were used to calibrate the soil hydraulic parameters (Table 1), and the $T1$ and $T3$ treatment data were used to validate the model and its optimized parameters. Since relatively similar trends in SWCs were obtained for the three treatments, the results only for the $T1$ treatment (validation) are presented in Fig. 6. Figure 6 documents that a relatively good agreement between experimental and simulated data was obtained. Overall, temporal changes in SWCs in the upper soil layers (0–10, 10–20, and 20–40 cm) were larger than in the deeper layers (40–60 and 60–100 cm), since these layers were more directly affected by irrigation, precipitation, evaporation, and transpiration. After all irrigation and rainfall events, SWCs increased quickly in the upper soil layers (0–40 cm), especially in the very top layers (0–20 cm), and mainly under the tomato and corn strips. On the other hand, SWC fluctuations in the bare strip were less dramatic, since this area was not directly affected by irrigation.

During the entire crop growth season, the mean relative errors (MRE) for all three treatments and all locations were smaller than 20 % (Table 3), with the average MRE for treatments $T1$, $T2$, and $T3$ being 10.7, 9.5, and 11.6 %, respectively. The root mean square errors (RMSE) for the three treatments were 0.043, 0.035, and 0.040 $cm^3\ cm^{-3}$, respectively. The average errors in upper layers were slightly larger than in deeper layers, reflecting higher SWC variations due to irrigation, precipitation, and root water uptake (Table 3). The lowest errors were obtained for the deepest soil layer of 60–100 cm. From these values, it could be concluded that SWCs simulated using HYDRUS (2D/3D) agreed well with those measured, and that HYDRUS (2D/3D) is well suited for simulating water contents in a drip-irrigated strip intercropping field under plastic mulch.

SWC differences between different locations

In Table 4 (for all three treatments) and Fig. 7 (only for treatment $T1$), we compare SWCs for a time period of drip irrigation between DOY 167 and DOY 220. Table 4 and Fig. 7 indicate that there were significant differences ($p < 0.05$) between SWCs at the $P1$, $P2$, and $P3$ locations in the top soil layers (0–10 and 10–20 cm), and that these differences gradually decreased with depth, especially for the bottom soil layer (60–100 cm) where no visible differences were observed. Although the overall trend in SWC variations was very similar for all three treatments during the growth period, it was obvious that there were differences in SWCs among different treatments due to different irrigation amounts in the upper soil layers. However, there were insignificant differences in SWCs in the deeper layers of 40–60 and 60–100 cm (Table 4; Fig. 7).

The SWCs in the main root region (0–40 cm) were highest at $P1$ and lowest at $P2$, and there were significant differences in SWCs at these three locations ($p < 0.01$). The SWCs at these three locations ($P1$, $P2$, and $P3$) were statistically different because of different flow processes at these locations, such as root water uptake, evaporation, and irrigation. The maximum difference in the SWC was observed between the $P1$ and $P2$ locations (Table 4), with the average SWC in the upper soil layer (0–40 cm) at the $P1$ location being about 30 % higher than at the $P2$ location. This was caused mainly by the absence of irrigation and mulch at the $P2$ (bare strip) location, especially during DOY 167–208 (Fig. 7). There was a competition for water and fertilizer uptake between the two crops.

Since there were very few roots in the deep root zone (40–100 cm) and the effect of irrigation there was negligible, this zone was largely affected by the shallow groundwater. Table 4 shows that the average SWCs were very similar at the three locations at depths of 60–100 cm, and that there were no statistically significant differences between $T1$ ($p = 0.720$), $T2$ ($p = 0.956$), and $T3$ ($p = 0.979$), because SWCs at these depths were almost unaffected by irrigation (see also Fig. 7).

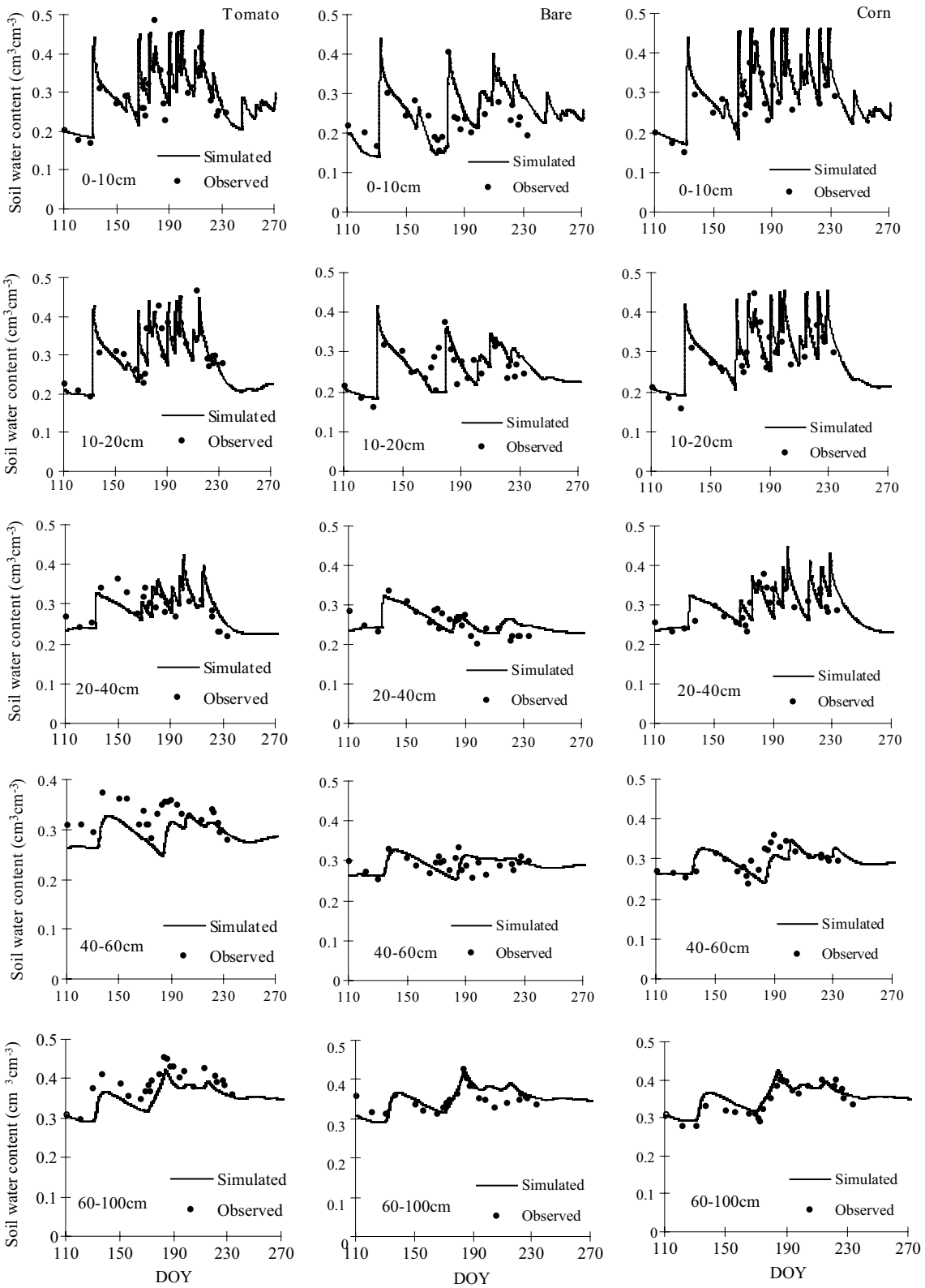

Fig. 6 Simulated and observed SWCs at *P*1 (under tomatoes, *left*), *P*2 (in the bare section, *middle*), and *P*3 (under corn, *right*) locations for treatment *T*1 at different depths

Table 3 Error analysis for different treatments (*T*1, *T*2, and *T*3) at different locations (*P*1, *P*2, and *P*3) and different depths

Depth (cm)/error		Treatment/location								
		*T*1			*T*2			*T*3		
		*P*1	*P*2	*P*3	*P*1	*P*2	*P*3	*P*1	*P*2	*P*3
0–10	MAE ($cm^3\ cm^{-3}$)	0.04	0.04	0.05	0.02	0.04	0.03	0.04	0.04	0.04
	MRE (%)	11.86	18.32	15.99	8.36	17.51	11.74	18.25	17.66	17.23
	RMSE ($cm^3\ cm^{-3}$)	0.05	0.05	0.07	0.03	0.04	0.05	0.05	0.05	0.06
10–20	MAE ($cm^3\ cm^{-3}$)	0.03	0.03	0.05	0.02	0.02	0.03	0.04	0.03	0.05
	MRE (%)	10.74	11.85	15.60	7.27	10.35	10.98	16.53	10.03	18.32
	RMSE ($cm^3\ cm^{-3}$)	0.05	0.04	0.07	0.03	0.03	0.04	0.05	0.03	0.06
20–40	MAE ($cm^3\ cm^{-3}$)	0.03	0.02	0.04	0.02	0.02	0.04	0.02	0.02	0.03
	MRE (%)	10.8	9.17	13.05	6.80	7.15	16.36	10.10	5.86	14.28
	RMSE ($cm^3\ cm^{-3}$)	0.04	0.03	0.05	0.02	0.02	0.05	0.03	0.02	0.04
40–60	MAE ($cm^3\ cm^{-3}$)	0.04	0.02	0.02	0.02	0.02	0.02	0.02	0.03	0.03
	MRE (%)	10.75	7.83	6.70	7.56	8.43	7.24	7.19	9.47	9.02
	RMSE ($cm^3\ cm^{-3}$)	0.04	0.03	0.03	0.03	0.03	0.03	0.03	0.04	0.03
60–100	MAE ($cm^3\ cm^{-3}$)	0.03	0.02	0.02	0.04	0.02	0.02	0.02	0.03	0.03
	MRE (%)	8.22	4.56	5.77	10.69	7.05	5.23	5.11	7.47	7.55
	RMSE ($cm^3\ cm^{-3}$)	0.04	0.02	0.02	0.05	0.03	0.02	0.02	0.04	0.03

Table 4 Simulated average SWCs ($cm^3\ cm^{-3}$) at different depths and locations (*P*1, *P*2, and *P*3), and for different treatments (*T*1, *T*2, and *T*3) between DOY 167 and DOY 220

Treatments/locations		Depths				
		0–10 cm	10–20 cm	20–40 cm	40–60 cm	60–100 cm
*T*1	*P*1	0.3657A	0.3358A	0.3084A	0.2980A	0.3740A
	*P*2	0.2490B	0.2585B	0.2451B	0.2960A	0.3740A
	*P*3	0.3627A	0.3292AB	0.3030A	0.2939A	0.3738A
*T*2	*P*1	0.3510A	0.3188A	0.2841A	0.2900A	0.3734A
	*P*2	0.2379B	0.2430B	0.2336B	0.2949B	0.3735A
	*P*3	0.3476AB	0.3114A	0.2778A	0.2840A	0.3732A
*T*3	*P*1	0.3312A	0.2965A	0.2533A	0.2885A	0.3736A
	*P*2	0.2322B	0.2345B	0.2289B	0.2944B	0.3736A
	*P*3	0.3278AB	0.2890AB	0.2477AB	0.2822A	0.3733A

Values followed by the same letter within a column are not significantly different at $p \leq 0.05$ according to Duncan's multiple range test

Two-dimensional soil water distributions

Two-dimensional soil water distributions (Fig. 8) for different irrigation treatments were analyzed to evaluate the movement of soil water in the root zone during the time period between DOY 214 and DOY 216 (i.e., after the sixth irrigation cycle). The SWCs increased 1 day after irrigation in all three treatments, especially in the top 0- to 30-cm-soil layer around the emitters. Because of a low amount of irrigation water, the infiltration front moved only about 30 cm in both vertical and horizontal directions from drip emitters.

When the soil water content is below the wilting point, it cannot be used any longer by crops (Allen et al. 1998). The soil water content at a wilting point is about 0.21 $cm^3\ cm^{-3}$ for a given soil texture according to the UNSODA database (Leij et al. 1996) and about 0.17–0.24 $cm^3\ cm^{-3}$ according to Allen et al. (1998). As a result, a severe "water stress zone" (with water contents near the wilting point) developed between the two drippers at a depth of about 30–40 cm. When the amount of irrigation water was reduced in treatments *T*2 and *T*3, the "water stress zone" increased in size. The size of the "water stress zone" was about 48 cm^2 in treatment *T*1 (evaluated using AutoCAD 2007 (Autodest Inc., USA) and simulated results), which resulted in a negligible stress on root water uptake (Fig. 8a). The "water stress zone" was about 530 cm^2 in treatment *T*2, which caused a slight restriction of the crop growth (Fig. 8c). On the other hand, this area was about 1134 cm^2 in treatment *T*3, which clearly affected the crop

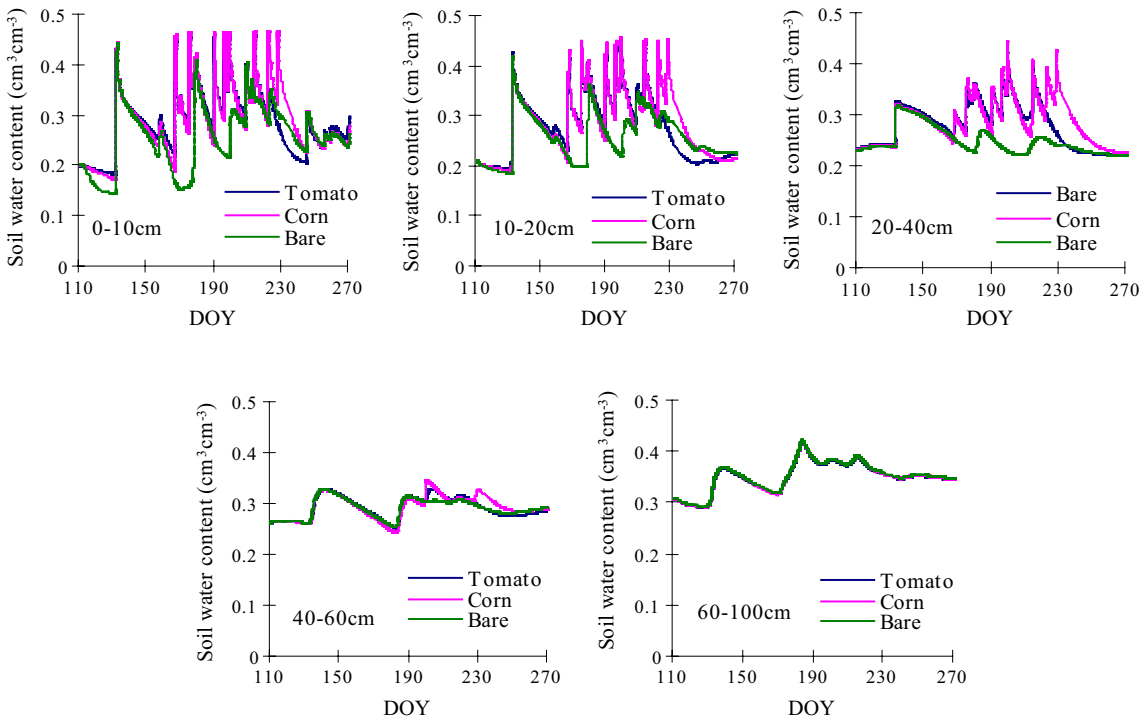

Fig. 7 A comparison of simulated SWCs at *P*1 (*tomato*), *P*2 (*bare*), and *P*3 (*corn*) locations at different depths for the *T*1 treatment

growth (Fig. 8e). However, since the SWC in soil layers below a depth of 60 cm was mainly influenced by the shallow groundwater, especially in the 80- to 100-cm-soil layer, there was almost no water stress on plant water uptake in this domain (Fig. 8a–f).

Numerical simulations indicate that the non-mulched region between two crop strips (i.e., the bare strip, *P*2) was little influenced by irrigation, and thus, the SWC was significantly lower in this region than in the two other strips. The "water stress zone" can be found in the bare strip (*P*2) for all three treatments. There was no water stress in other strips (*P*1 and *P*3) for treatment *T*1. However, the water stress was found for both tomatoes (*P*1) and corn (*P*3) strips in treatments *T*2 and *T*3. The water stress in the *P*3 strip was higher than in the *P*1 strip because of higher transpiration and root water uptake in the corn strip. During soil water redistribution, 2 days after irrigation, the SWCs gradually increased at the *P*2 position and did not affect the crop growth any longer in this region for treatment *T*1 (Fig. 8b). However, a small "water stress zone" could be found in the non-mulched region for treatment *T*2 (Fig. 8d). In treatment *T*3, the water stress was significant (Fig. 8f), indicating that the irrigation was not sufficient either. Figure 8 also shows that the effect of irrigation on the SWC is in all three treatments very low at depths below 40 cm and almost none below the depth of 60 cm where only about 3.4 % of the total root mass can be found. Consequently, almost identical SWC was found at these depths in all three treatments.

Conclusion

The HYDRUS (2D/3D) model was parameterized and calibrated to simulate the soil water movement in a drip-irrigated, strip intercropping field under plastic mulch. Simulated SWCs at observation points at different locations and for different irrigation treatments were found to be in good agreement with experimental data. The average errors were all lower than 20 %, while the average MREs were 10.7, 9.5, and 11.6 %, and the average RMSEs were 0.043, 0.035, and 0.040 $cm^3\ cm^{-3}$ for irrigation treatments *T*1, *T*2, and *T*3, respectively.

SWCs were significantly affected by irrigation amounts, and significant differences in SWCs were observed between different locations. There were also significant differences in SWCs in the shallow root region (0–40 cm) between *P*1 (highest water contents), *P*2 (lowest water contents), and *P*3 locations. SWC differences at different locations gradually decreased with depth, and there were no visible differences in the deep root region (40–100 cm). Additionally, the SWCs in the non-mulched region (location *P*2) were similar for all treatments. The average SWC in the shallow root region was largely influenced

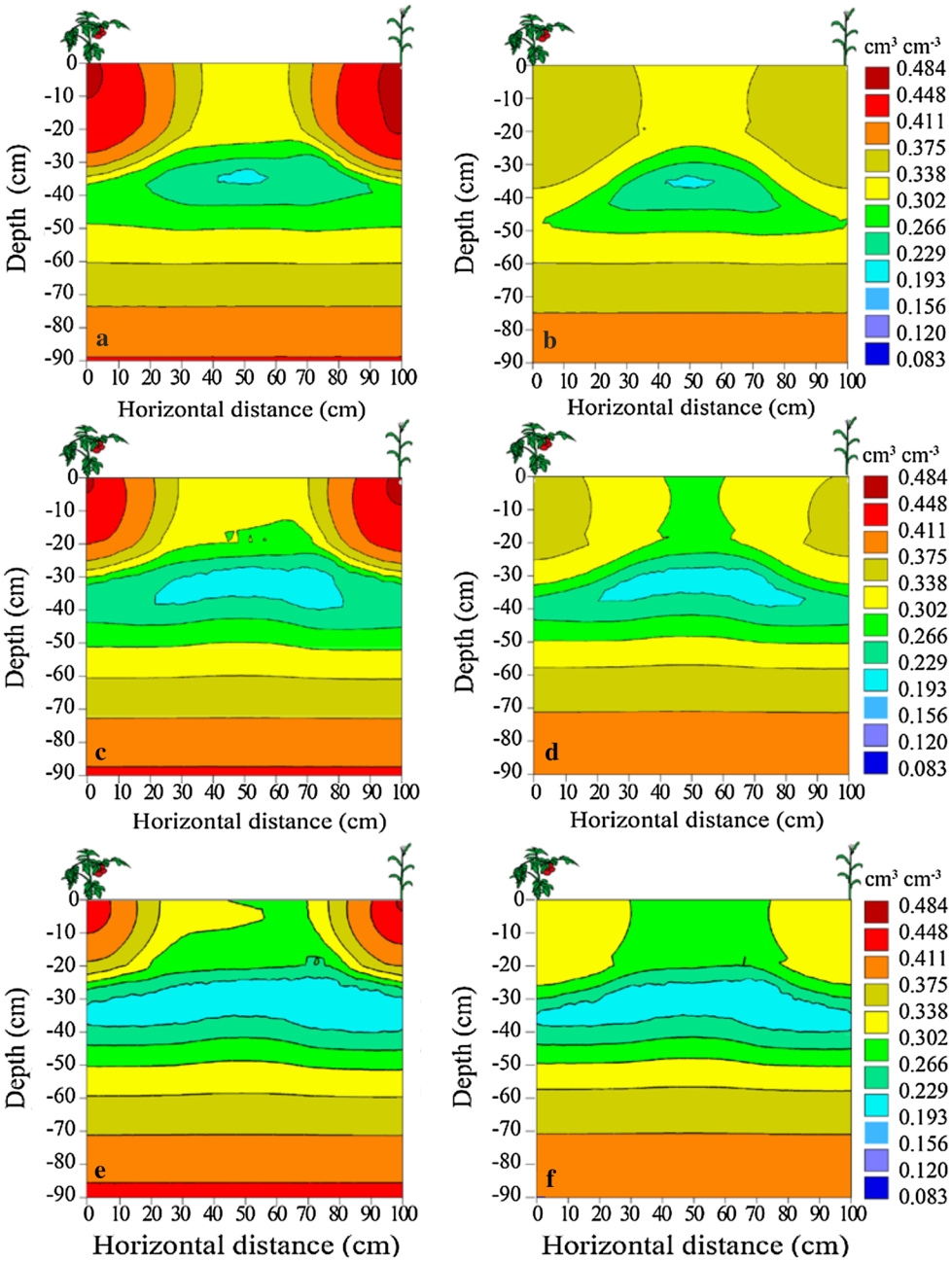

Fig. 8 Two-dimensional soil water distributions after the sixth irrigation cycle for the *T*1 (*top*; **a**, **b**), *T*2 (*middle*; **c**, **d**), and *T*3 (*bottom*; **e**, **f**) treatments; 1 day after irrigation (*left*; **a**, **c**, **e**) and 2 days after irrigation (*right*; **b**, **d**, and **f**)

by irrigation. The higher the irrigation amounts used, the higher the SWCs observed.

The analysis of two-dimensional soil water content distributions revealed that the soil water distributions were affected by irrigation and root distributions. A severe "water stress zone" (with water contents near the wilting point) appeared in the 30- to 40-cm-soil layer, located mainly in the non-mulched region (the bare strip) in a drip-irrigated intercropping field under plastic mulch. The size of the "water stress zone" increased with decreasing irrigation, and it reached 1134 cm^2 for the lowest irrigation amount (*T*3 treatment). Water redistribution following irrigation increased the SWCs in the crop strips and reduced the water stress in this area compared to the bare strip. The optimal soil water distribution pattern in the root zone of the intercropping field can be easily maintained using separate drip emitter lines for each crop. However, low irrigation amounts would still cause water stress in crop strips. Although redistribution of water following irrigation gradually reduced this stress for treatment *T*2 after about 2 days, for treatment *T*3, the water stress remained present even after water redistribution.

The numerical model HYDRUS (2D/3D) proved to be a powerful tool for investigating dynamics of soil water in a

drip-irrigated intercropping field under plastic mulch. Fully calibrated model could be used to quickly evaluate different irrigation management strategies without the need for a laborious field work. However, much work needs to be done to design optimal irrigation strategies, such as irrigation frequencies, emitter depths, and emitter rates (e.g., Kandelous et al. 2012) for these complex conditions. Additional modifications of HYDRUS (2D/3D), such as considerations of root growth for multiple crops; the surface energy balance; and coupled movement of water, vapor, and energy, would also be greatly beneficial for such analysis.

Acknowledgments This research was jointly supported by the Innovation Team Program of Educational Ministry (IRT13069), the National Natural Science Foundation of China (51109105, 51349003, and 51469022), the State Science and Technology Support Program (2011BAD29B03), the Post-Doctor Foundation of China (2011M500547, 2012T50250), Natural Sciences Foundation of Inner Mongolia, and the Program for Young Talents of Science and Technology in Universities of Inner Mongolia Autonomous Region (NJYT-12-B10).

References

Abou Lila TS, Berndtsson R, Persson M, Somaida M, Ei-Kiki M, Hamed Y, Mirdan A (2013) Numerical evaluation of subsurface trickle irrigation with brackish water. Irrig Sci 31:1125–1137

Allen R, Pereira LS, Raes D, Smith M (1998) Crop evapotranspiration: guidelines for computing crop requirements. FAO Irrigation and Drainage Paper No. 56, FAO, Rome

Arbat G, Puig-Bargués J, Duran-Ros M, Barragán J, Ramírez de Cartagena F (2013) Drip-irriwater: computer software to simulate soil wetting patterns under surface drip irrigation. Comput Electron Agric 98:183–192

Assouline S, Möller M, Cohen S, Ben-Hur M, Grava A, Narkis K, Siber A (2006) Soil-plant system response to pulsed drip irrigation and salinity: Bell pepper case study. Soil Sci Soc Am J 70:1556–1568

Awal MA, Koshi H, Ikeda T (2006) Radiation interception and use by maize/peanut intercrop canopy. Agric For Meteorol 139:74–83

Badr AE, Abuarab ME (2013) Soil moisture distribution patterns under surface and subsurface drip irrigation systems in sandy soil using neutron scattering technique. Irrig Sci 31:317–332

Booltink HWG, Bouma J, Giménez D (1991) Suction crust infiltrometer for measuring hydraulic conductivity of unsaturated soil near saturation. Soil Sci Soc Am J 55:566–568

Burt CM, Isbell B (2005) Leaching of accumulated soil salinity under drip irrigation. Trans ASAE 48:2115–2121

Campbell GS, Norman JM (1989) The description and measurement of plant canopy structure. Plant canopies: their growth form, and function. Society for experimental biology. Cambridge University Press, Cambridge, pp 1–19

Cavero J, Plant RE, Shennan C, Williams JR, Kiniry JR, Benson VW (1998) Application of EPIC model to nitrogen cycling in irrigated processing tomatoes under different management systems. Agric Syst 56(4):391–414

Cook FJ, Torburn PJ, Fitch P, Bristow KL (2003) wetup: a software tool to display approximate wetting patterns from drippers. Irrig Sci 22:129–134

Cote CM, Bristow KL, Charlesworth PB, Cook FJ, Thorburn PJ (2003) Analysis of soil wetting and solute transport in subsurface trickle irrigation. Irrig Sci 22:143–156

Dabach S, Lazarovitch N, Šimůnek J, Shai U (2013) Numerical investigation of irrigation scheduling based on soil water status. Irrig Sci 31:27–36

Dabach C, Shani U, Lazarovitch N (2015) Optimal tensiometer placement for high-frequency subsurface drip irrigation management in heterogeneous soils. Agric Water Manag 152:91–98

De Silva MS, Nachabe MH, Šimůnek J, Carnahan R (2008) Simulating root water uptake from a heterogeneous vegetative cover. J Irrig Drain Eng 134(2):167–174

Dhima KV, Lithourgidis AS, Vasilakoglou IB, Dordas CA (2007) Competition indices of common vetch and cereal intercrops in two seeding ratio. Field Crops Res 100:249–256

Doltra J, Muñoz P (2010) Simulation of nitrogen leaching from a fertigated crop rotation in a Mediterranean climate using the EU-Rotate_N and Hydrus-2D models. Agric Water Manag 97:277–285

Feddes R, Kowalik P, Zaradny H (1978) Simulation of field water use and crop yield. Wiley, New York

Gao Y, Duan AW, Qiu XQ, Liu ZG, Sun JS, Zhang JP, Wang HZ (2010) Distribution of roots and root length density in a maize/soybean strip intercropping system. Agric Water Manag 98:199–212

Hopmans JW, Šimůnek J, Romano N, Durner W (2002) Inverse modeling of transient water flow. In: Dane JH and Topp GC (eds) Methods of soil analysis, part 4, physical methods, chapter 3.6.2, 3rd edn. SSSA, Madison, WI, pp 963–1008

Hussein F, Janat M, Yakoub A (2011) Assessment of yield and water use efficiency of drip-irrigated cotton (*Gossypium hirsutum* L.) as affected by deficit irrigation. Turk J Agric For 35:611–621

Ityel E, Lazarovitch N, Silberbush M, Ben-Gal A (2011) An artificial capillary barrier to improve root zone conditions for horticultural crops: physical effects on water content. Irrig Sci 29:171–180

Kandelous MM, Šimůnek J, van Genuchten MTh, Malek K (2011) Soil water content distributions between two emitters of a subsurface drip irrigation system. Soil Sci Soc Am J 75(2):488–497

Kandelous MM, Kamai T, Vrugt JA, Šimůnek J, Hanson B, Hopmans JW (2012) Evaluation of subsurface drip irrigation design and management parameters for alfalfa. Agric Water Manag 109:81–93

Keller J, Bliesner RD (1990) Sprinkle and trickle irrigation. Van Nostrand Reinhold, New York

Lazarovitch N, Šimůnek J, Ben-Gal A, Shani U (2007) Uniqueness of soil hydraulic parameters determined by a combined wooding inverse approach. Soil Sci Soc Am J 71(3):860–865

Lazarovitch N, Pollton M, Furman A, Warrick AW (2009) Water distribution under trickle irrigation predicted using artificial neural networks. J Eng Math 64:207–218

Leij FJ, Alves WJ, van Genuchten MTh, Williams JR (1996) Unsaturated Soil Hydraulic Database, UNSODA 1.0 user's manual. Rep. EPA/600/R96/095. USEPA, Ada, OK

Lindquist JL, Arkebauer TJ, Walters DT, Cassman KG, Dobermann A (2005) Maize radiation use efficiency under optimal growth conditions. Agron J 97:72–78

Liu MX, Yang JS, Li XM, Yu M, Wang J (2013) Numerical simulation of soil water dynamics in a drip irrigated cotton field under plastic mulch. Pedosphere 23(5):620–635

Makumba W, Janssen B, Oenema O, Akinnifesi FK, Mweta D, Kwesiga F (2006) The long-term effects of a gliricidia–maize intercropping system in Southern Malawi, on gliricidia and maize yields, and soil properties. Agric Ecosyst Environ 116(1–2):85–92

Neuman SP, Feddes RA, Bresler E (1974) Finite element simulation of flow in saturated-unsaturated soils considering water uptake by plants, Third Annual Report, Project No. A10-SWC-77, Hydraulic Engineering Lab., Technion, Haifa, Israel

Parajulee MN, Montandon R, Slosser JE (1997) Relay intercropping to enhance abundance of insect predators of cotton aphid (*Aphis gossypii Glover*) in Texas cotton. Int J Pest Manag 43:227–232

Philip JR (1984) Travel times from buried and surface infiltration point sources. Water Resour Res 20(7):990–994

Richards L (1931) Capillary conduction of liquid in porous media. Physics 1:318–333

Rowe EC, Noordwijk MV, Suprayogo D, Cadisch G (2005) Nitrogen use efficiency of monoculture and hedgerow intercropping in the humid tropics. Plant Soil 268:61–74

Sampathkumar T, Pandian BJ, Mahimairaja S (2012) Soil moisture distribution and root characters as influenced by deficit irrigation through drip system in cotton–maize cropping sequence. Agric Water Manag 103:43–53

Schaap MG, Leij FJ, van Genuchten MTh (2001) Rosetta: a computer program for estimating soil hydraulic parameters with hierarchical pedotransfer functions. J Hydrol 251:163–176

Schader C, Zaller JG, Kopke U (2005) Cotton-basil intercropping: effects on pests, yields and economical parameters in an organic field in Fayoum, Egypt. Biol Agric Hortic 23:59–72

Šimůnek J, van Genuchten MTh, Šejna M (2006) The HYDRUS software package for simulating two- and three-dimensional movement of water, heat, and multiple solutes in variably saturated media, Technical manual, version 1.0, PC Progress, Prague, Czech Republic, p 241

Šimůnek J, van Genuchten MTh, Šejna M (2008) Development and applications of the HYDRUS and STANMOD software package and related codes. Vadose Zone J 7(2):587–600

Singh M, Singh UB, Ram M, Yadav A, Chanotiya CS (2013) Biomass yield, essential oil yield and quality of geranium (*Pelargonium graveolens* L. Her.) as influenced by intercropping with garlic (*Allium sativum* L.) under subtropical and temperate climate of India. Ind Crop Prod 46:234–237

Skaggs TH, Trout TJ, Šimůnek J, Shouse PJ (2004) Comparison of Hydrus-2D simulations of drip irrigation with experimental observations. J Irrig Drain Eng 130(4):304–310

Skaggs TH, Trout TJ, Rothfuss Y (2010) Drip irrigation water distribution patterns: effects of emitter rate, pulsing, and antecedent water. Irrig Sci 74:1886–1896

Tanwar SPS, Rao SS, Regar PL, Datt S, Kumar P, Jodha BS, Santra P, Kumar R, Ram R (2014) Improving water and land use efficiency of fallow-wheat system in shallow Lithic Calciorthid soils of arid region: introduction of bed planting and rainy season sorghum–legume intercropping. Soil Till Res 138:44–55

van Genuchten MTh (1980) A closed-form equation for predicting the hydraulic conductivity of unsaturated soils. Soil Sci Soc Am J 44:892–898

Wang ZM, Jin MG, Šimůnek J, van Genuchten MTh (2014) Evaluation of mulched drip irrigation for cotton in arid Northwest China. Irrig Sci 32:15–27

Wesseling JG, Brandyk T (1985) Introduction of the occurrence of high groundwater levels and surface water storage in computer program SWATRE, Nota 1636, Institute for Land and Water Management Research (ICW). Wageningen, The Netherlands

Xu X, Huang GH, Qu ZY, Pereira LS (2010) Assessing the groundwater dynamics and impacts of water saving in the Hetao Irrigation District, Yellow River basin. Agric Water Manag 98:301–313

Yaghi T, Arslan A, Naoum F (2013) Cucumber (*Cucumis sativus*, L.) water use efficiency (WUE) under plastic mulch and drip irrigation. Agric Water Manag 128:149–157

Zhang FS, Li L (2003) Using competitive and facilitative interactions in intercropping systems enhances crop productivity and nutrient-use efficiency. Plant Soil 248:305–312

Zhang L, van der Werf W, Zhang S, Li B, Spiertz JHJ (2007) Growth, yield and quality of wheat and cotton in relay strip intercropping systems. Field Crops Res 103:178–188

Zhou QY, Kang SZ, Zhang L, Li FS (2007) Comparison of APRI and Hydrus-2D models to simulate soil water dynamics in a vineyard under alternate partial root zone drip irrigation. Plant Soil 291:211–223